



ELSEVIER

Physica E 13 (2002) 80–88

PHYSICA E

www.elsevier.com/locate/physa

Plasmons and the drag effect in a strong magnetic field

A. Manolescu^a, B. Tanatar^{b, *}

^aNational Institute of Materials Physics, P.O. Box MG-7 Bucharest-Magurele, Romania

^bDepartment of Physics, Bilkent University, Bilkent, 06533 Ankara, Turkey

Received 11 December 2000; received in revised form 5 May 2001; accepted 27 June 2001

Abstract

We study the effect of magnetoplasmons on the drag resistance in a strong magnetic field, at finite temperatures. The typical magnetic field is about 1 T, and the temperature is up to 10 K. The Landau levels are broadened by disorder, but well separated in energy. We discuss intra-Landau level magnetoplasmons, with low frequencies, below ω_c , and inter-Landau level magnetoplasmons (also called Bernstein modes), with high frequencies, close to multiples of ω_c . We compare the temperature dependence of the minima and maxima of the Shubnikov–de Haas oscillations of the transresistance. © 2002 Published by Elsevier Science B.V.

PACS: 73.02.Mf; 73.50.Dn; 73.50.Jt

Keywords: Drag effect; Magnetoplasmons; Disorder; Strong magnetic field

1. Introduction

Coulomb drag is an interesting transport effect stemming from many-body interactions between two systems of charge carriers in close proximity. More specifically, we can consider a typical experimental situation of two two-dimensional (2D) electron gases parallel to each other and separately contacted. When one of the layers is subjected to an external current, the electrons in the other layer are dragged because of the long-range Coulomb forces. In practice no

current is allowed to flow in the second layer and the so-called drag voltage is measured (for recent review see Ref. [1]). The experiments performed on GaAs double quantum well electron and electron–hole systems [2–5] measure the transresistance in different temperature regimes. The effect of phonons, plasmon excitations, and disorder have been studied.

In the presence of a magnetic field perpendicular to the 2D electron gases, the situation becomes even richer because of the interplay between screening, disorder, and magnetic field effects, as well as the possibility of probing the quantum Hall effect regimes. The experimental results of Hill et al. [6] and Rubel et al. [7] revealed an interesting double peak structure in transresistivity which was theoretically

* Corresponding author. Tel.: +90-312-2901591;
fax: +90-312-2664579.

E-mail address: tanatar@fen.bilkent.edu.tr (B. Tanatar).

predicted by Bønsager et al. [8,9]. Patel et al. [10] and Feng et al. [11] found negative drag in the regime of the fractional quantum Hall effect, when the upper Landau level of one layer is more than half-filled while the other is less than half-filled, which was argued to be a consequence of disorder and the existence of the holelike dispersion relation. Theoretical work [8,9,12–14] on magnetodrag was devoted to understand the magnetic field and temperature dependence of transresistance in a broad range of parameters. Coulomb drag measurements in the integer and fractional quantum Hall effect region are also reported [11,15] leading to an intense theoretical activity [16–21].

In this paper we revisit the effect of magnetoplasmons on the drag resistivity under strong magnetic fields. It is known that the plasma oscillations increase the interaction between the two electron layers, both in the absence [22–25], and in the presence [8,9,12–14] of a magnetic field. In particular, in magnetic field, the plasma oscillations have many modes, and thus their role becomes more complicated. Bønsager et al. [8,9] did not study the structure of the plasma oscillations. This was to some extent done by Wu et al. [12] who discuss the splitting due to the interaction between the two electron layers. Recently, Khaetskii and Nazarov [13,14] derived analytic expressions for the transresistance, capturing the combined plasmon and disorder effects for several situations with moderate magnetic fields.

The effect of the plasmons on the transresistance is however very implicit, captured in spectral integrations, and difficult to understand. In addition to the mentioned works, in the present paper we perform numerical calculations, and we distinguish the variation of the transresistance stemming from the magnetoplasmons, by cutting off the corresponding peaks of the inverse dielectric function. We use the approach proposed in Refs. [8,9]. We also wish to make a clear distinction between the collective modes generated by the single-particle excitations between different Landau levels, also known as Bernstein magnetoplasmons, and the collective modes generated by single-particle transitions within the same Landau level. The Bernstein (interlevel) modes have frequencies given by multiples of the cyclotron frequencies, while the intralevel modes have frequencies below the cyclotron frequency. Thus, the enhancement of

the transresistance at low temperatures is due to the intralevel modes.

In the rest of the paper, we first outline the formalism to calculate the drag resistivity in the presence of a perpendicular magnetic field and disorder. We then analyze the contribution of magnetoplasmons in various examples for a range of parameters. We conclude with a brief summary.

2. The drag resistance

The Coulomb drag rate for double-layer systems has been derived through a variety of theoretical approaches [1,22–25] ranging from memory function formalism, Boltzmann transport theory, to diagrammatic perturbation theory methods. Our starting point is the formula for the transresistance derived by Bønsager et al. [8,9] given as

$$\rho_D = -\frac{\hbar^2}{2e^2} \frac{1}{n_1 n_2 T} \int \frac{d^2 q}{(2\pi)^2} q^2 \times \int_0^\infty \frac{d\omega}{2\pi} \left| \frac{u_{12}(q)}{\varepsilon_{12}(q, \omega)} \right|^2 \frac{\text{Im} \chi_1(q, \omega) \text{Im} \chi_2(q, \omega)}{\sinh^2(\hbar\omega/2T)}. \quad (1)$$

Here n_1 and n_2 denote the electron densities in the layers 1 and 2, respectively, and T is the temperature in energy units, $u_{12} = 2\pi e^2/(\kappa q) \exp(-qd)$ is the Fourier transform of the Coulomb-interaction potential of the electrons in one layer with those in the other layer, κ being the dielectric constant of the semiconductor material and d the distance between the two layers. χ_1 and χ_2 are the individual susceptibilities (density response functions) of the electron layers, and $\varepsilon_{12}(q, \omega)$ is the dielectric function of the coupled layers, in the random-phase approximation (RPA),

$$\varepsilon_{12}(q, \omega) = \varepsilon_1(q, \omega)\varepsilon_2(q, \omega) - u_{12}^2(q) \chi_1(q, \omega) \chi_2(q, \omega). \quad (2)$$

Also in the RPA, the single-layer dielectric function is

$$\varepsilon_{1,2}(q, \omega) = 1 - u(q)\chi_{1,2}(q, \omega), \quad (3)$$

where $u(q) = 2\pi e^2/(\kappa q)$. As we shall discuss below $\chi_{1,2}(q, \omega)$ appearing in the above expressions are functions of temperature T , and magnetic field B .

3. Landau level broadening, dielectric susceptibility, and magnetoplasmons

To include the broadening of the Landau levels due to impurities, we use the Green functions

$$G_n^\pm(E) = \frac{1}{E - E_n - \Sigma^\pm(E)}, \quad (4)$$

where $E_n = (n + 1/2)\hbar\omega_c$ is the energy of the Landau level n , $n = 0, 1, 2, \dots$, $\omega_c = eB/m_{\text{eff}}$ is the cyclotron frequency, and $\Sigma^-(E) = (\Sigma^+(E))^*$ is the self-energy associated with the interaction of the electrons with impurities. Here we consider $\Sigma(E)^\pm$ a simple complex number (and not a true operator), i.e. independent of the Landau level index n . This ansatz corresponds to the self-consistent Born approximation (SCBA), with a delta-function model for the electron-impurity interaction potential, which leads to the equation [26,27]

$$\Sigma^-(E) = \Gamma^2 \sum_n \frac{1}{E - E_n - \Sigma^-(E)}, \quad (5)$$

where Γ is the characteristic energy of the disorder, proportional to the square root of the magnetic field,

$$\Gamma = \gamma\sqrt{B} = \hbar \left(\frac{\omega_c}{2\pi\tau} \right)^{1/2}, \quad (6)$$

with τ the classical relaxation time. The regime of strong magnetic fields is defined by $\omega_c\tau = (\hbar\omega_c/\Gamma)^2 / (2\pi) \gg 1$. The density of states is written as

$$D(E) = D_0 \frac{\hbar\omega_c}{\pi} \sum_n \text{Im} G_n^-(E), \quad (7)$$

where $D_0 = m_{\text{eff}}/(\pi\hbar^2)$, and it is shown in Fig. 1 for a typical situation of interest. In this scheme all the Landau levels have the same energy broadening, $\Delta = 4\Gamma$. The material parameters are chosen for GaAs, $m_{\text{eff}} = 0.067m_e$, $\kappa = 12.4$, and we assume spin degeneracy.

The single-layer dielectric susceptibility is given by (we omit here the layer index)

$$\begin{aligned} \chi(q, \omega) = & \frac{1}{\pi\ell^2} \sum_{n,m \geq 0} \left[E_{nm} \left(\frac{(q\ell)^2}{2} \right) \right]^2 \\ & \times \int \frac{dE}{\pi} \mathcal{F}(E) \text{Im} G_n^-(E) \\ & \times [G_m^+(E - \hbar\omega) + G_m^-(E + \hbar\omega)], \end{aligned} \quad (8)$$

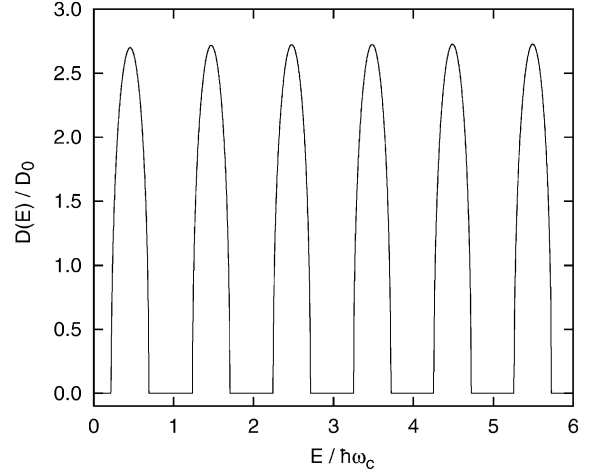


Fig. 1. A typical density of states for the first six Landau levels. Here $B = 0.94$ T, and $\gamma = 0.2$ (meV T) $^{-1/2}$, see Eqs. (5–7).

where \mathcal{F} is the Fermi function, $\ell = \sqrt{\hbar/eB}$ is the magnetic length, and

$$\begin{aligned} E_{nm}(z) = & \left(\frac{m!}{n!} \right)^{1/2} z^{(n-m)/2} e^{-z/2} L_m^{n-m}(z) \\ = & (-1)^{m-n} E_{mn}(z), \end{aligned} \quad (9)$$

with $L_n^m(x)$ the associated Laguerre polynomials [28]. Eq. (8) is the polarization loop (also known as Lindhard formula), but with Green functions dressed with the electron-impurity self energy, here within the SCBA given by Eq. (5). We thus neglect the corresponding vertex corrections. The matrix elements of the vertex functions can be written as $E_{nm}(q^2\ell^2/2)\{1 + \mathcal{O}(\zeta^2)\}$, where $\zeta = E_{nm}(q^2\ell^2/2)\Gamma/\hbar\omega_c$ as given by Bønsager et al. [8,9]. As long as the Landau level broadening is not too large, $\zeta^2 \ll 1$ and the vertex corrections can be ignored. Also $E_{nm}(q^2\ell^2/2) \lesssim 1$ for our range of wave vectors. For more discussion on the vertex corrections see also Refs. [8,9,13,14].

If the energy-dependent self-energy, Eq. (5), is reduced to a constant adiabatic parameter η , and $\eta \rightarrow 0$, Eq. (8) becomes

$$\begin{aligned} \chi(q, \omega) = & \frac{1}{\pi\ell^2} \sum_{n,m \geq 0} \left[E_{nm} \left(\frac{(q\ell)^2}{2} \right) \right]^2 \\ & \times \frac{\mathcal{F}(E_n) - \mathcal{F}(E_m)}{E_n - E_m - \hbar\omega + i\eta}, \end{aligned} \quad (10)$$

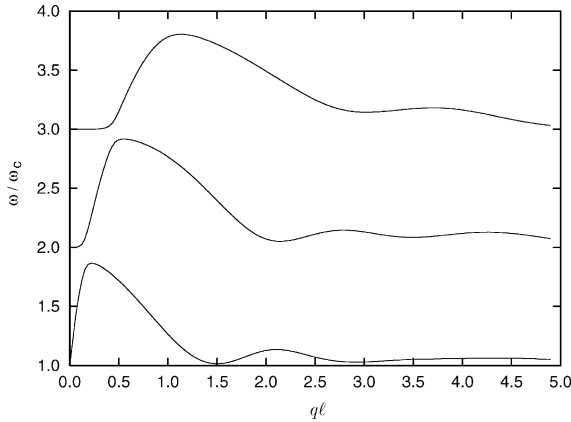


Fig. 2. The dispersion relation for the first three Bernstein modes. Here $B = 1.1$ T, and the electron density is $1.8 \times 10^{11} \text{ cm}^{-2}$.

which is a form quite often used for describing the electromagnetic absorption in quantum nanostructures in strong magnetic fields [29]. In Eq. (10) we see only the inter Landau level (virtual) transitions, $n \neq m$, contributing to the dielectric response. The plasma oscillations, with dispersion $\omega(q)$ obtained from $\varepsilon(q, \omega) = 0$, form a series of modes, known as Bernstein modes, with frequencies given by multiples of cyclotron frequency, $|m - n|\omega_c$, plus an electric blue shift. Such dispersion laws are shown in Fig. 2. In the present context we shall call the Bernstein plasmons *inter-level* modes. In the limit $q \rightarrow 0$, the lowest Bernstein mode has the well-known dispersion relation $\omega(q) = (\omega_c^2 + 2\pi n e^2 q / \kappa m_{\text{eff}})^{1/2}$.

Suppose the Landau levels have no disorder broadening. In this case an *intralevel* component of the dielectric response, i.e. given by single-particle transitions within the same Landau level, can be obtained only in the static regime, $\omega = 0$, by assuming thermodynamic equilibrium [30,31] (isothermal response). It consists of an extra term in Eq. (10) for $\omega = 0$,

$$\chi_{\text{intra}}(q) = -\frac{1}{\pi \ell^2} \sum_n \left[E_{nm} \left(\frac{(q\ell)^2}{2} \right) \right]^2 \frac{\partial \mathcal{F}(E_n)}{\partial \mu}, \quad (11)$$

where μ is the chemical potential. This component of the dielectric susceptibility is responsible for the nonlinear screening and the appearance of the compressible and incompressible edge strips in the two-dimensional electron gas in strong magnetic fields, at low temperatures [32].

A nontrivial treatment of the disorder effect, as in Eq. (8), combined with the broadening of the Landau levels, allows however both intralevel and interlevel types of dielectric response, at *finite* frequencies, $\omega \neq 0$. The intralevel collective excitations have frequencies $\omega < \omega_c$, whereas the interlevel modes have $\omega > \omega_c$. Because of damping, described by $\text{Im} \chi(q, \omega)$, the plasma oscillations are no longer zeros of $\varepsilon(q, \omega)$. However they can be seen as peaks of $1/|\varepsilon(q, \omega)|$, around the frequencies where both $\text{Re} \varepsilon$ and $\text{Im} \varepsilon$ vanish. This is shown in Fig. 3(a), for one layer, with the parameters mentioned in the caption. The peak of $1/|\varepsilon(q, \omega)|$ at $\omega \approx 0.5\omega_c$ corresponds to the intralevel mode, and those at $\omega \approx 1.7\omega_c$ and $\omega \approx 2.6\omega_c$ to the first two interlevel (Bernstein) modes. The height of the peaks depends on q and on the magnetic field. In particular, the height of the intralevel peak also depends on the filling factor ν : it reaches a maximum when μ is in the middle of a Landau level, i.e. close to an odd ν (6.8 in our example), and vanishes for even values, when μ goes into an energy gap, if the temperature is much lower than the gap width. The frequency is approximately equal to the width of the Landau level, $\Delta/\hbar = 0.44\omega_c$. In Fig. 3(b) we repeat the same plot with an increased disorder, from $\gamma = 0.2 \text{ (meV T)}^{-1/2}$ to $\gamma = 0.3 \text{ (meV T)}^{-1/2}$. The plasmon peaks decrease, as expected. Although the real and imaginary parts of the dielectric function do not change very much, they no longer vanish at close frequencies (or they may not vanish at all for an even stronger disorder).

In Fig. 3(c) we show the inverse dielectric function for the double layer, Eq. (2), corresponding to Fig. 3(a). We take $d = 25 \text{ nm}$ for the layer separation, which is fixed for all calculations. Each mode of a single layer splits into *two* modes of the coupled layers, one with the charge in each layer oscillating in phase and the other one out-of-phase [12]. The higher the frequency, the bigger the splitting, such that the splitting of the intralevel mode is not clearly resolved for our parameters, and only a small lateral shoulder can be observed in Fig. 3(c). Furthermore, the dispersion of the intralevel peak of $|\varepsilon_{12}^{-1}(\omega, q)|$ can be seen in Fig. 3(d), as a function of both ω and q . The collective mode merges rapidly into the single-particle excitation background and vanishes with increasing

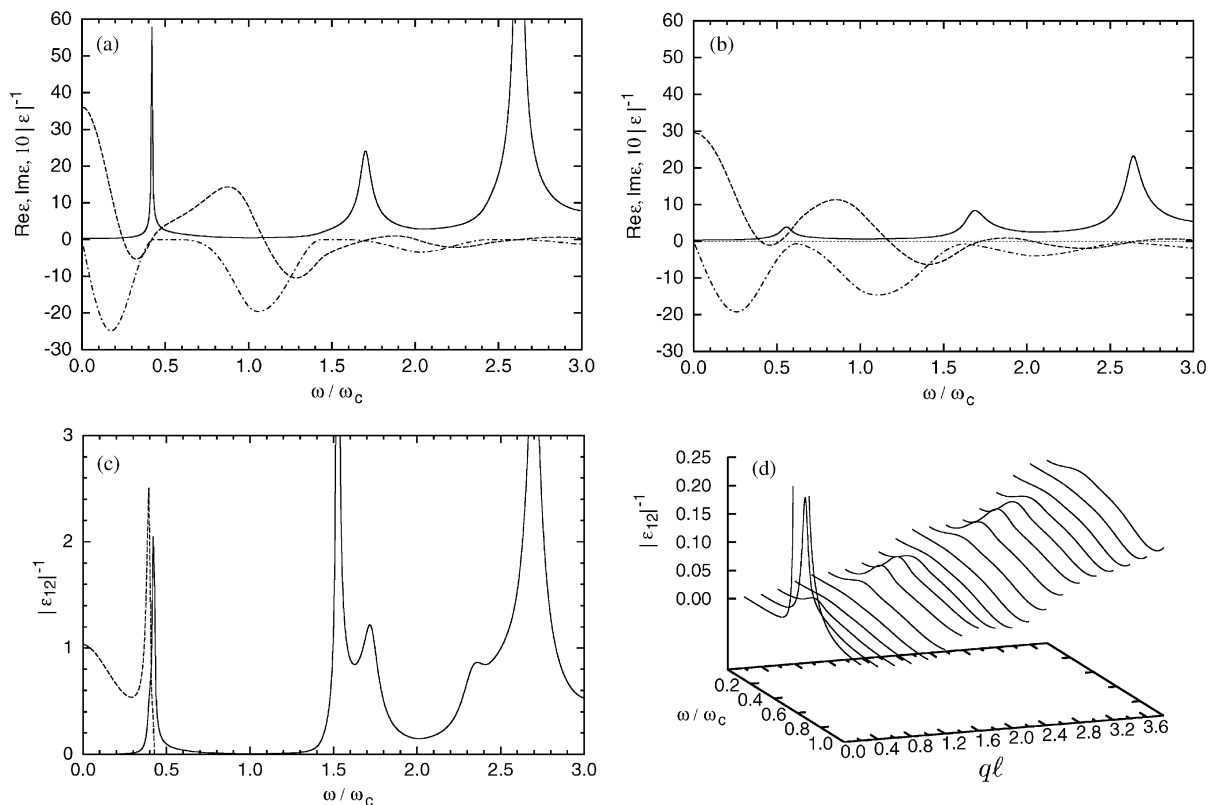


Fig. 3. The dielectric function, for $B = 1.1$ T, $n_1 = n_2 = 1.8 \times 10^{11}$ cm $^{-2}$, $q = 0.3/\ell$, $T = 1.5$ K, and $d = 25$ nm. (a) For a single layer, $\text{Re } \varepsilon(q, \omega)$ with the dashed line, $\text{Im } \varepsilon(q, \omega)$ with the dashed–dotted line, $1/|\varepsilon(q, \omega)|$ with the full line and multiplied by 10, with the disorder parameter $\gamma = 0.2$ (meV T) $^{-1/2}$; the thin dotted line shows the zero axis; (b) the same, but with $\gamma = 0.3$ (meV T) $^{-1/2}$; (c) The inverse dielectric function for the double layer, with the full line, and also, in arbitrary units, the integrand of the q -integration of Eq. (1), with the dashed line, both corresponding to $\gamma = 0.2$ (meV T) $^{-1/2}$; (d) A detailed dispersion of $1/|\varepsilon_{12}(q, \omega)|$ of (c) around the intralevel peak.

wave vector. As mentioned before, the intralevel peak vanishes for integer filling factors, at low temperatures, but it may still develop with increasing temperature.

4. The magnetoplasmons and the transresistance

In Fig. 3(c) we also show the integrand in the q -integral of Eq. (1) as a function of ω . The function $1/\sinh^2(\hbar\omega/2T)$ decays exponentially for $\hbar\omega > T$. Although here $T/\hbar\omega_c = 0.068$, the real frequency cut-off is shifted to much higher values, because of the intralevel peak which increases the effective dynamically screened interaction in Eq. (1). Therefore, even at experimentally low temperatures, one

expects the influence of magnetoplasmons on the transresistance, and thus a nontrivial increase with T [8,9,12–14].

In Fig. 4 we show the analog of the Shubnikov–de Haas (SdH) oscillations, for the transresistance, for several temperatures. They reflect the oscillations of the density of states, shown in Fig. 1, but through the dissipative part of the susceptibility, $\text{Im } \chi(q, \omega)$, at low frequencies. In Fig. 4(a) we fixed the disorder parameter, and we varied the temperature. When the magnetic field increases, as long as the Fermi level is inside a Landau level, the intralevel electrostatic screening (determined by the dielectric susceptibility given in Eq. (11)), also increases, and thus the effective interlayer coupling decreases. This is the explanation for the slight minima inside the rightmost SdH

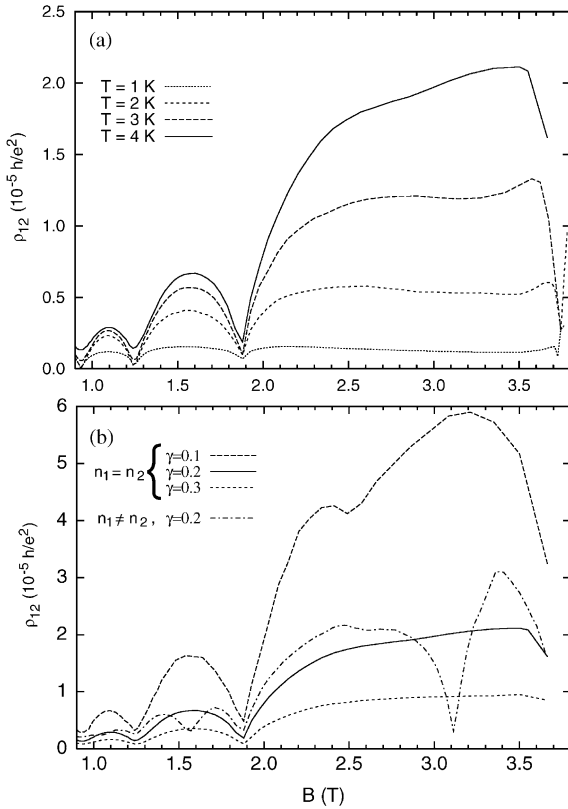


Fig. 4. The Shubnikov–de Haas oscillations of the transresistance ρ_{12} . (a) For temperatures between 1 and 4 K. $n_1 = n_2 = 1.8 \times 10^{11} \text{ cm}^{-2}$ and $\gamma = 0.2 \text{ (meV T)}^{-1/2}$. The leftmost minimum corresponds to $\nu = 8$ and the rightmost to $\nu = 2$. (b) For a fixed temperature, $T = 4 \text{ K}$, but with three disorder parameters. (see the legend). The solid and dashed lines are for the same densities as in Fig. 4(a). The dash-dotted line is for different electron densities, $n_1 = 1.8 \times 10^{11}$ and $n_2 = 1.5 \times 10^{11} \text{ cm}^{-2}$.

peaks. This effect has been calculated in detail [8,9] and observed in experiments [6,7].

In Fig. 4(b) the temperature is fixed, $T = 4 \text{ K}$, and the disorder parameter is varied. As expected from the evolution of the plasmon peaks of the dielectric function with the disorder parameter, the transresistance decreases with increasing disorder. Such behavior is opposite to that of the ordinary magnetoresistance, which increases with increasing disorder. In Fig. 4(b) we also show a trace for different single-layer electron densities, $n_1 \neq n_2$, with the dash-dotted line. Deep minima are observed for the magnetic fields corresponding to integer filling factors in

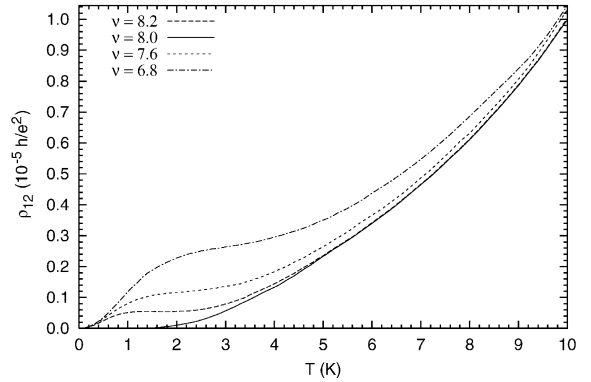


Fig. 5. The temperature dependence of the transresistance for various positions in the SdH oscillations, corresponding to slightly different values of the magnetic field: $\nu = 8.2$ ($B = 0.911 \text{ T}$), $\nu = 8.0$ ($B = 0.934 \text{ T}$), $\nu = 7.6$ ($B = 0.983 \text{ T}$), $\nu = 6.8$ ($B = 1.1 \text{ T}$). The other parameters are the same as in Fig. 4(a).

each layer separately, much deeper than the minima produced by the screening effect. (For the electron density of $1.8 \times 10^{11} \text{ cm}^{-2}$ we have $\nu B = 7.47 \text{ T}$, and for $1.5 \times 10^{11} \text{ cm}^{-2}$ we have $\nu B = 6.23 \text{ T}$.)

The temperature dependence of the SdH maxima and minima is qualitatively different at low temperatures, because of the presence, and respectively the absence of the intralevel dissipation at odd, and respectively at even filling factors. In other words, the negative peaks of $\text{Im } \epsilon_1(q, \omega)$ and $\text{Im } \epsilon_2(q, \omega)$, for $\omega < \omega_c$, see the dash-dotted lines of Figs. 3(a), (b), vanish for integer filling factors, and therefore the transresistance is suppressed at low temperatures, according to Eq. (1). This is shown in Fig. 5 for $\nu = 8$. Slightly changing the magnetic field towards a SdH maximum, e.g. to $\nu = 8.2$ or to $\nu = 7.6$ the transresistance is strongly enhanced at low temperatures by the presence of intralevel dissipation, and also by the low-frequency plasmons. The effect of the Bernstein modes appears at $T \approx 3\text{--}4 \text{ K}$, enhancing the interlayer effective Coulomb interaction, and consequently the transresistance ρ_{12} increases nonlinearly. The onset of the intralevel plasmons is in the vicinity of the first inflexion point on the curves in Fig. 5, and the interlevel modes start playing a role close to the second inflexion point.

In order to better understand the contribution of the magnetoplasmons in the transresistance, we have cut

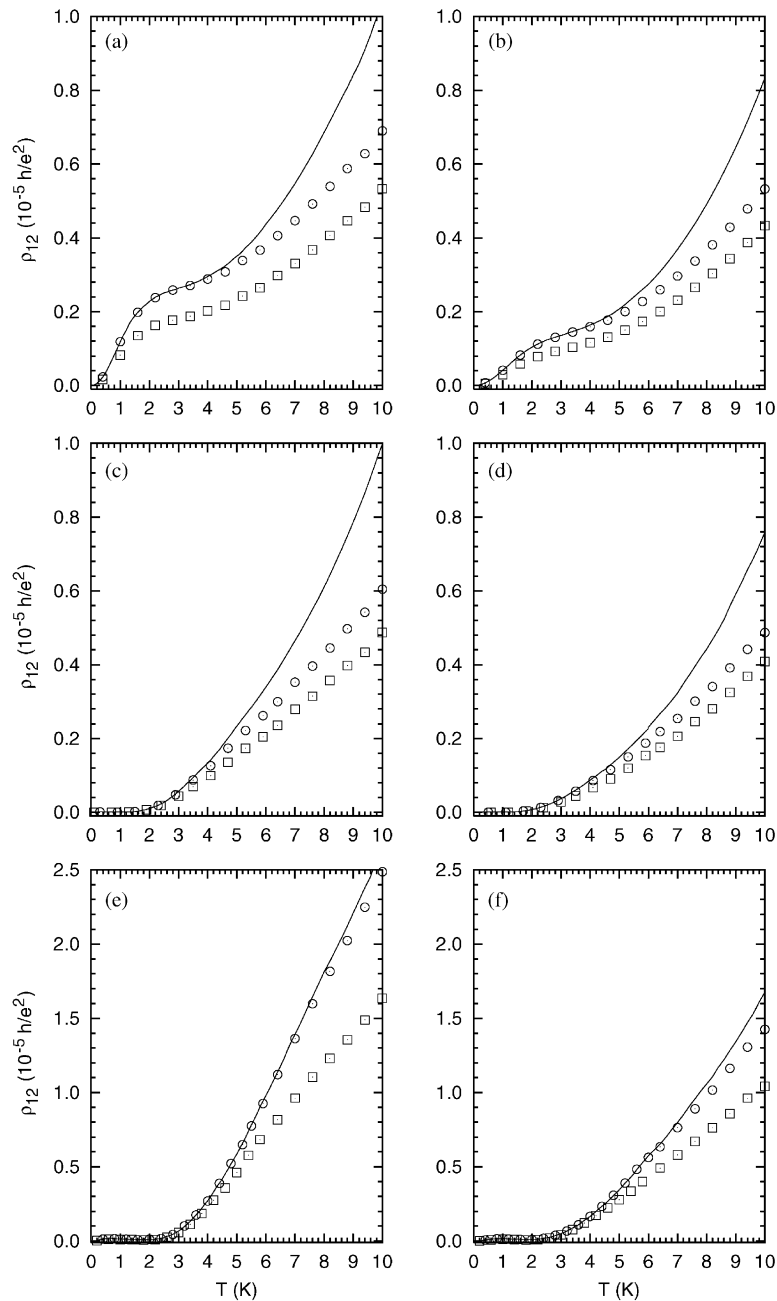


Fig. 6. The temperature dependence of the transresistance, with and without the collective modes as a function of temperature. The solid lines indicate results including the plasmons, squares these after excluding all plasma modes, and circles after excluding only the interlevel modes, with a cutoff $\alpha = 0.05$. The parameters are as follows. (a) $n_1 = n_2 = 1.8 \times 10^{-11} \text{ cm}^{-2}$, $\nu = 6.8$ ($B = 1.1 \text{ T}$), $\gamma = 0.2 \text{ (meV T)}^{-1/2}$; (b) like (a), but with $\gamma = 0.3$; (c) and (d) like (a) and (b), but for $\nu = 8.0$ ($B = 0.934 \text{ T}$); (e) for different densities, $n_1 = 1.8 \times 10^{-11} \text{ cm}^{-2}$, $n_2 = 1.5 \times 10^{-11} \text{ cm}^{-2}$, with $B = 1.867 \text{ T}$, ($\nu_1 = 4, \nu_2 = 3.3$), corresponding to a minimum of ρ_{12} , see the dash-dotted line of Fig. 4(b); (f) like (e), for $\gamma = 0.3$.

the peaks of the inverse dielectric function $\varepsilon_{12}^{-1}(q, \omega)$ in the numerical integration of Eq. (1), by replacing $\varepsilon_{12}^{-1}(q, \omega)$ with $\min[\alpha, \varepsilon_{12}^{-1}(q, \omega)]$, with $\alpha = 0.05$. The results are displayed in Fig. 6 for various parameters. With squares we show the numerical results for ρ_{12} with cutoff for all frequencies, i.e. removing all the plasma modes, and with circles with cutoff only for $\omega > \omega_c$, i.e. removing only the Bernstein modes. Evidently, such a procedure does not remove only the plasma modes, but also some effects of the single-particle excitations, see for instance Fig. 3(d). For comparison we have considered in Fig. 6 two values of the disorder parameter, consistent with the previous examples. As expected, with increasing disorder the effect of the collective modes becomes weaker. For integer filling factors, Fig. 6(c) and (d), the intralevel modes do not exist at low temperatures, so we see no change in the transresistance for $T < 3$ K when we remove all peaks (the traces with squares), but we see an effect at higher temperatures. Indeed, removing only the interlevel modes, the deviations from the complete results is smaller on our temperature interval (the traces with circles).

Finally, in Fig. 6(e) and (f) we show results for different densities, corresponding to a minimum of the Shubnikov–de Haas oscillations at $B = 1.867$ T, shown in Fig. 4(b) with the dash-dotted line. Although only the filling factor for one layer is integer ($\nu_1 = 4.0, \nu_2 = 3.3$), the temperature dependence of ρ_{12} is similar to that when both filling factors are integer. Of course, the absence of the dissipation in one layer, $\text{Im} \varepsilon_1(q, \omega) = 0$, is enough to suppress the transresistance, according to Eq. (1). Due to the higher cyclotron frequency, the effect of the Bernstein modes can be observed only at temperatures higher than those in the previous examples.

5. Summary and conclusions

In summary, we have calculated numerically the transresistance and we have illustrated with several examples the effect of magnetoplasmons at low temperatures and a high magnetic field such that only a few Landau levels are populated. With increasing temperature, but still in the experimentally low-temperature regime, first the intralevel, and then the interlevel magnetoplasmons, increase the effective

Coulomb coupling between the electron layers, and hence the transresistance. The temperature dependence of the minima and of the maxima of the SdH oscillations is completely different, because of the presence and absence, respectively, of the intralevel dielectric response. We have discussed how transresistance decreases with increasing disorder which in our model calculations taken to be the broadening parameter. To find out the effect of the collective modes we have introduced a cutoff parameter in the numerical calculations of the transresistance. For the temperature range considered, we find an increase of the transresistance up to 50% due to the magnetoplasma modes.

Acknowledgements

This work was partially supported by the Scientific and Technical Research Council of Turkey (TUBITAK) under Grant No. TBAG-2005, by NATO under Grant No. SfP971970, and by the Turkish Department of Defense under Grant No. KOBRA-001. A.M. acknowledges the support and hospitality at ICTP and Bilkent University where parts of this work was done. We appreciate useful discussions with Professor Vidar Gudmundsson.

References

- [1] A.G. Rojo, *J. Phys.: Condens. Matter* 11 (1999) R31.
- [2] T.J. Gramila, J.P. Eisenstein, A.H. MacDonald, L.N. Pfeiffer, K.W. West, *Phys. Rev. Lett.* 66 (1991) 1216.
- [3] P.M. Solomon, P.J. Price, D.J. Frank, D.C. La Tulipe, *Phys. Rev. Lett.* 63 (1989) 2508.
- [4] U. Sivan, P.M. Solomon, H. Shtrikman, *Phys. Rev. Lett.* 68 (1992) 1196.
- [5] N.P.R. Hill, J.T. Nicholls, E.H. Linfield, M. Pepper, D.A. Ritchie, G.C.A. Jones, B.Y.-K. Hu, K. Flensberg, *Phys. Rev. Lett.* 78 (1997) 2204.
- [6] N.P.R. Hill, J.T. Nicholls, E.H. Linfield, M. Pepper, D.A. Ritchie, A.R. Hamilton, G.A.C. Jones, *J. Phys.: Condens. Matter* 8 (1996) L557.
- [7] H. Rubel, A. Fischer, W. Dietsche, K. von Klitzing, K. Eberl, *Phys. Rev. Lett.* 78 (1997) 1763.
- [8] M.C. Bónsager, K. Flensberg, B.Y.-K. Hu, A.-P. Jauho, *Phys. Rev. Lett.* 77 (1996) 1366.
- [9] M.C. Bónsager, K. Flensberg, B.Y.-K. Hu, A.-P. Jauho, *Phys. Rev. B* 56 (1997) 10314.
- [10] N.K. Patel, E.H. Linfield, K.M. Brown, M. Pepper, D.A. Ritchie, G.A.C. Jones, *Semicond. Sci. Technol.* 12 (1997) 309.

- [11] X.G. Feng, S. Zelakiewicz, H. Noh, T.J. Ragucci, T.J. Gramila, L.N. Pfeiffer, K.W. West, *Phys. Rev. Lett.* 81 (1998) 3219.
- [12] M.W. Wu, H.L. Cui, N.J.M. Horing, *Mod. Phys. Lett. B* 10 (1996) 279.
- [13] A.V. Khaetskii, Y.V. Nazarov, *Phys. Rev. B* 59 (1999) 7551.
- [14] A.V. Khaetskii, Y.V. Nazarov, *Physica B* 256–258 (1998) 220.
- [15] M.P. Lilly, J.P. Eisenstein, L.N. Pfeiffer, K.W. West, *Phys. Rev. Lett.* 80 (1998) 1714.
- [16] Y.B. Kim, A.J. Millis, *Physica E* 4 (1999) 171.
- [17] F. Zhou, Y.B. Kim, *Phys. Rev. B* 59 (1999) 7825.
- [18] I. Ussishkin, A. Stern, *Phys. Rev. Lett.* 81 (1998) 3932.
- [19] A. Stern, I. Ussishkin, *Physica E* 1 (1997) 176.
- [20] S. Sakhi, *Phys. Rev. B* 56 (1997) 44098.
- [21] E. Shomshoni, S.L. Sondhi, *Phys. Rev. B* 49 (1994) 11484.
- [22] L. Zheng, A.H. MacDonald, *Phys. Rev. B* 48 (1993) 8203.
- [23] A.-P. Jauho, H. Smith, *Phys. Rev. B* 47 (1993) 4420.
- [24] H.C. Tso, P. Vasilopoulos, F.M. Peeters, *Phys. Rev. Lett.* 68 (1992) 2516.
- [25] K. Flensberg, B.Y.-K. Hu, *Phys. Rev. B* 52 (1995) 14796.
- [26] R.R. Gerhardts, J. Hajdu, *Z. Phys. B* 245 (1971) 126.
- [27] T. Ando, A.B. Fowler, F. Stern, *Rev. Mod. Phys.* 54 (1982) 437.
- [28] I.S. Gradshteyn, I.M. Ryzhik, *Table of Integrals, Series, and Products*, Academic Press, New York, 1980.
- [29] V. Gudmundsson, R.R. Gerhardts, *Phys. Rev. B* 54 (1996) R5223.
- [30] V. Gudmundsson, R.R. Gerhardts, *Solid State Commun.* 67 (1988) 845.
- [31] U. Wulf, V. Gudmundsson, R.R. Gerhardts, *Phys. Rev. B* 38 (1988) 4218.
- [32] D.B. Chklovskii, B.I. Shklovskii, L.I. Glazman, *Phys. Rev. B* 46 (1992) 4036.